ARTICLES

Molecular Dynamics Study of Translational and Rotational Diffusion in Liquid Ortho-terphenyl

R. J. Berry,*,† D. Rigby,‡ D. Duan,† and M. Schwartz*,§

Air Force Research Laboratory, Materials and Manufacturing Directorate, Wright−Patterson AFB, Ohio 45433, Accelrys, Inc., 10188 Telesis Court, San Diego, California 92121, and Department of Chemistry, University of North Texas, Denton, Texas 76203

Received: July 11, 2005; In Final Form: November 8, 2005

NVT molecular dynamics simulations were performed on liquid *o*-terphenyl as a function of temperature in the range 320−480 K. Computed translational diffusion coefficients displayed the non-Arrhenius behavior expected of a fragile glass-forming liquid and were in good, semiquantitative agreement with experimental results. Rotational correlation functions calculated for various vectors within the molecule exhibited a very short time (0−1 ps) initial decay, followed by a reversal, which corresponds to free reorientation within the "solvent" cage prior to collision with a wall. Rotational correlation times of three orthogonal vectors fixed on the central benzene were close to equal at all temperatures, indicating nearly isotropic overall molecular reorientation. The average correlation times exhibited a non-Arrhenius temperature dependence and were in very good agreement with experimental values derived from ^{2}D and ^{1}H NMR relaxation times. Correlation times of vectors located on the lateral phenyl rings were used to calculate the "spinning" internal rotation diffusion coefficients, which were approximately twice as great as the overall rotational diffusion constants, indicating rapid internal rotation of the phenyl side groups over wide ranges of angle in the liquid.

Introduction

Because *o*-terphenyl (OTP) possesses a small dipole moment (0.24 D) and low partial charges on the carbons and hydrogens, it belongs to the class of glass-forming liquids classified by Angell as fragile glass formers.[1−3] In these fluids, the principal interaction between molecules is via van der Waals forces, and it has been observed experimentally that the temperature dependence of their viscosity and transport properties (e.g., translational and rotational diffusion coefficients) exhibit large deviations from Arrhenius behavior. As the prototypical fragile glass former, OTP has generated great interest over the years, and there have been numerous experimental investigations of its properties by methods including NMR[4−6] and dielectric[7,8] relaxation, dynamic light scattering,[9−14] and inelastic neutron scattering.[15−18] NMR relaxation and light scattering are particularly valuable techniques to study glass-forming liquids because the motional dynamics can be investigated over very large time scales (>5 decades) and down to temperatures within a few degrees of T_g.[5,12] There have also been a number of excellent investigations by Ediger, Sillescu, and others (e.g., refs 19−24) of the translational and rotational dynamics of probe molecules in OTP, which have revealed that (not surprisingly) the dynamics of the probes are size dependent and may be very different from that of OTP itself.

Unlike experimental techniques such as NMR relaxation and light-scattering line shapes, molecular dynamics simulations of motional dynamics in glass-forming liquids such as OTP are comparatively limited in the time scale accessible to the technique (∼2 decades) due to the dramatic increase in the characteristic times (translational and rotational) at temperatures approaching T_g (vide infra). On the other hand, one has the capability to obtain a much more detailed picture of molecular details of the motions, including internal rotation, from the simulations than can be readily extracted from the experiments.

There have been a number of molecular dynamics simulations of the static and dynamic behavior of liquid OTP.[25−30] However, most of these simulations have not used completely atomistic force fields, and there has been little attention paid to the rotational dynamics in OTP.

With the goal of acquiring a better assessment of the capability of molecular dynamics simulations to replicate the non-Arrhenius behavior and provide semiquantitative estimates of the transport properties of fragile glass-forming liquids, we have performed simulations of the motional dynamics of OTP at temperatures ranging from 320 to 480 K in the liquid.

Computational Methods

Simulations were performed using the Accelrys[31] Discover molecular dynamics program and associated software modules. The Accelrys COMPASS[32−35] force field, designed to yield accurate values for both gas- and liquid-phase properties, was used for all the simulations. COMPASS is a completely

* To whom correspondence should be addressed.
† Wright−Patterson Air Force Base.
‡ Accelrys, Inc.
§ University of North Texas.

10.1021/jp053797v CCC: $33.50
Published on Web 12/14/2005

atomistic Class II force field, and the potential-energy function contains valence terms involving bond lengths, angles, and dihedrals + cross terms. As with other modern force fields, there are also out-of-plane terms designed to maintain planarity in aromatic systems such as the benzene rings in OTP. Other than terms in the potential-energy function, no further constraints were applied to the molecules (i.e., bond lengths, ring geometries, etc., were not frozen). As discussed in the original references,[32−35] the nonbond parameters were optimized to reproduce molar volumes and enthalpies of vaporization in a suite of test molecules under ambient conditions (usually 298 K and 1 atm. pressure), in which hydrocarbons were represented by benzene and toluene.[34]

Cubic cells containing 50 OTP molecules were built at 480 K and then equilibrated using NPT dynamics (Anderson thermostat and Berendsen barostat) at $P = 1$ atm. Equilibrated cells at lower temperatures were obtained by successive cooling at 20 K intervals down to 320 K, with 2 ns of NPT equilibration at each temperature. Simulations were also performed below 320 K. However, the translational and rotational dynamics below 320 K were too slow to permit extraction of useful data.

The cells equilibrated at each temperature and $P = 1$ atm were then used as the starting point for production runs using NVT dynamics (Berendsen thermostat), with sharp 10 Å cutoffs and periodic boundary conditions. These simulations were performed for periods of 4−15 ns, depending on temperature. The time step was 1 fs, and snapshots of the trajectories were stored every 1 ps. To investigate the short-time dynamics, NVT simulations were also performed at several temperatures for a period of 5 ps, with frames stored every 0.02 ps.

Results and Discussion

A. Intramolecular Torsion. Twisting of the two ancillary phenyl groups about the bond connecting them to the central benzene is an important component of OTP internal dynamics. To see whether the COMPASS force field properly characterizes the intramolecular geometry and motion, we have performed several calculations. The minimized (i.e., 0 K) structure of an isolated (gas-phase) molecule has a twist angle, $\phi = 47°$. Rotational dynamics performed at 400 K on the isolated molecule yielded a dihedral angle distribution peaking at ∼50−55°, and the distribution in the 400 K liquid-phase dynamics (50 molecule) has a maximum at ∼47−51°. The trends are consistent in that one expects a somewhat greater dynamical dihedral angle due to asymmetry of the torsional PES, i.e., a much higher barrier at $\phi = 0°$ (planar conformation) than at 90°.

The crystal structure exhibits two torsional angles at $\phi = 42$ and 62°.[36,37] However, more relevant to fluid phases are values of the gas-phase torsional angle. There are no accurate microwave or electron diffraction studies of OTP due to its low vapor pressure. However, there are a number of experimental or computational estimates: 48° (from gas-adsorption chromatography),[38] 55° (from molar Kerr constants; liquid),[39] 63° (from HeI photoelectron spectrum),[40] 54° (from intramolecular potential derived from crystal data + MM; isolated molecule),[41] 52° (B3LYP Calculation),[42] 54° (AM1 Calculation),[42] and 48° (INDO calculation).[43] One can see, therefore, that the twist angles computed by minimization and dynamics using COMPASS are consistent with the broad range of experimental estimates.

There is an experimental measurement of the torsional vibrational frequency from the liquid-phase Raman spectrum;[44] $\nu_{tors} \approx 70$ cm^{-1}, which is somewhat higher than our value of 51 cm^{-1}, determined by vibrational analysis on the isolated molecule. However, one expects the torsional frequency in the liquid to be higher than in the gas due to the presence of intermolecular steric repulsions. Furthermore, our value is in close agreement with the frequency predicted by the quantum mechanical B3LYP/6-31G(d) method:[42] $\nu_{tors} = 52$ cm^{-1}.

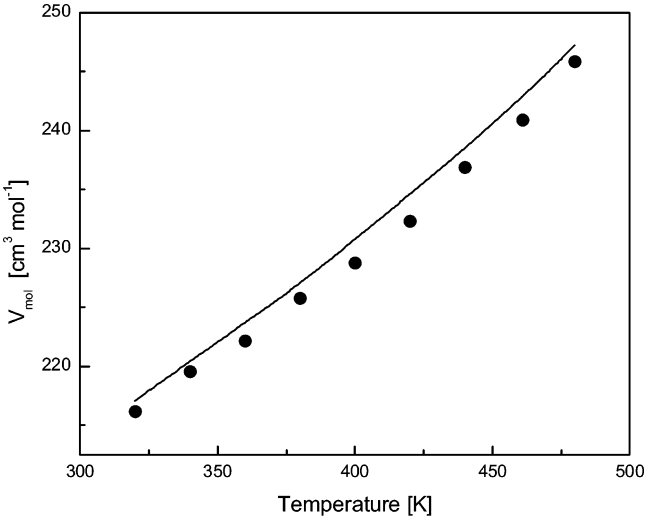

Figure 1. Experimental and calculated molar volumes. Line, experimental (refs 45 and 46); circles, calculated.

TABLE 1: Calculated Molar Volumes, Cohesive Energy Densities, and Enthalpies of Vaporization

temperature (K)	V_m (cm^3 mol^{-1})	CED (10^8 J m^{-3})	$\Delta_{vap}H°$ (kJ m^{-1})
320	216.2	4.10	91.1
340	219.6	3.92	88.9
360	222.2	3.78	87.2
380	225.8	3.68	84.9
400	228.8	3.46	83.2
420	232.3	3.29	81.3
440	236.9	3.18	79.0
461	240.9	3.03	77.1
480	245.9	2.89	74.8

B. Molar Volume and Enthalpy of Vaporization. Since the force field was parametrized to yield exact predictions of molar volume and enthalpy of vaporization only for the simplar hydrocarbons benzene and toluene at a single state point,[32−35] it is of interest to examine the transferability of the parameters to more complex aromatics such as the polyaromatic liquid, OTP, over a broad temperature range.

Computed molar volumes (from the 2-ns NPT runs at each temperature) are given in Table 1 and plotted in Figure 1, together with values of V_{mol} derived from experimental densities.[45,46] Uncertainties in V_{mol} were approximately ±0.2% at the 95% confidence level (∼2 standard errors). It was found that the agreement with experiment is extremely good, with deviations ≤1% at all temperatures. Simulations by one of the authors have shown that computed molar volumes are insensitive to both system size and nonbonded cutoff distance.[47]

Table 1 also contains the computed cohesive energy densities (CED) and derived enthalpies of vaporization ($\Delta_{vap}H° = V_{mol}$·CED + RT), as a function of temperature. The $\Delta_{vap}H°$ values are also plotted in Figure 2, together with experimental enthalpies from four reported studies of experimental OTP vapor pressures.[48−51] Enthalpies of vaporization were computed from the Antoine equation constants characterizing vapor pressures in the experimental references. The investigation by Sasse et al.[48] contains data over a temperature range (343−462 K), which closely overlaps the range in this investigation (320−480 K).

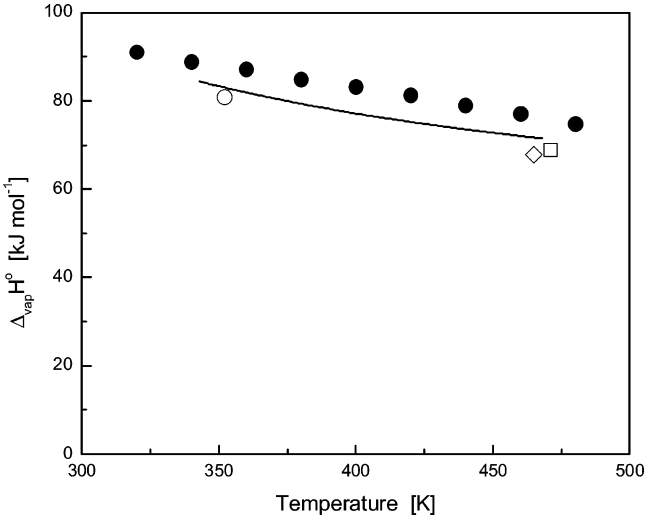

Figure 2. Experimental and calculated enthalpies of vaporization. Filled circles, calculated in this work; solid curve, experimental (ref 48); open circles, experimental (ref 49); open diamonds, experimental (ref 50); open square (ref 51).

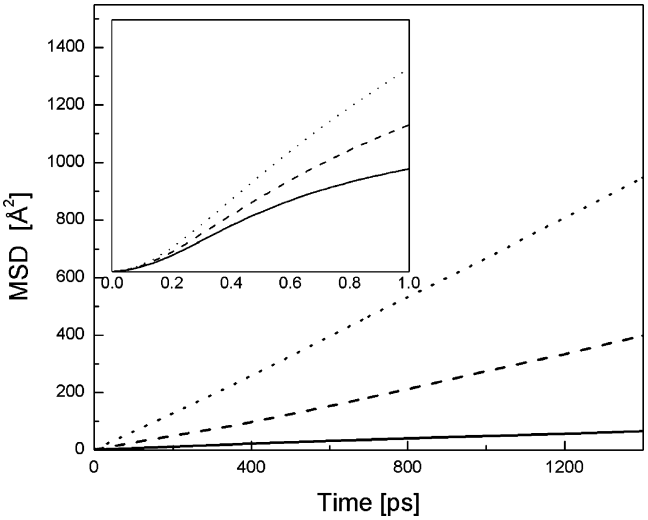

Figure 3. MSDs. Solid line, $T = 340$ K; dashed line, $T = 400$ K; dotted line, $T = 460$ K. The inset shows the short time behavior of the MSDs.

These data are represented by the solid curve in the figure. The temperature ranges of the other three studies have much less overlap (20−30 K) with our results (ref 49, 335−368 K; ref 50, 450−650 K; ref 51: 462−660 K). Hence, these data are represented by single points at the midpoint of the temperature overlap.

One may observe from the figure that the various experimental data are consistent and that the enthalpies of vaporization computed from the MD simulations are in qualitative agreement with experiment; deviations from values derived from the vapor pressures of Sasse et al.[48] are within 7−8% at all temperatures in the overlapping range. Furthermore, the average slope of the MD results ($d(\Delta_{vap}H°)/dT = -0.099$ kJ/mol K) is almost identical to that from the data in ref 48 (−0.105). Interestingly, the slope of the vaporization enthalpy curve estimated from group additivity considerations[52] ($d(\Delta_{vap}H°)/dT = -0.106$ kJ/mol K) is quite close to both the molecular dynamics and experimental values.

It should be noted that differences between calculated and experimentally deduced heats of vaporization are somewhat higher for OTP than for a number of simpler aromatic hydrocarbons containing one and two phenyl rings, which tend to be in the range of 0−2.5% around the normal boiling points.[47] Consequently a critical evaluation of both the simulation-derived and experimental data is desirable.

C. Translational Diffusion. The time dependence of the mean squared displacement (MSD $= \langle|\mathbf{r}(t) - \mathbf{r}(0)|^2\rangle$) of the molecular center of mass, averaged over all molecules and multiple time origins, were computed at each temperature. The MSDs at three representative temperatures are displayed in Figure 3. As expected, there is an initial "ballistic" regime from ∼0.5−0.8 ps (inset), corresponding to unhindered translation within the cage of other molecules, after which the MSD becomes linear in time. It is straightforward to determine the translational diffusion coefficient (D_{tr}) from the linear region of the plot via the Einstein relation, $\langle r^2(t)\rangle = 6D_{tr}t$.

Values of D_{tr} as a function of temperature are displayed in Table 2 and on a semilogarithmic inverse temperature plot (Figure 4). The figure also contains the reported experimental diffusion coefficients in OTP.[4] It is satisfying to note that the diffusion coefficients computed from the molecular dynamics simulations exhibit the same non-Arrhenius temperature dependence found experimentally in OTP and other fragile glass-forming liquids. In contrast, in a recent investigation of the non-glass-forming liquid, benzene,[53] translational diffusion coefficients were found to exhibit no deviations from Arrhenius behavior over the complete liquid range. In addition, the computed values are in very good semiquantitative agreement with experiment,

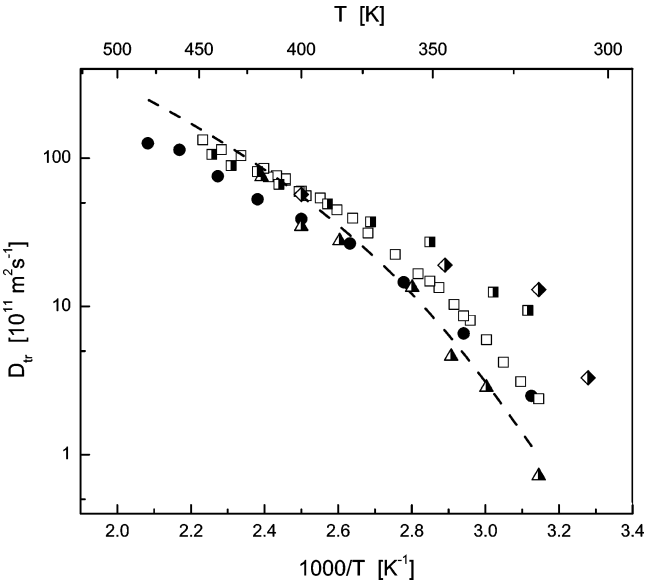

Figure 4. Translational diffusion coefficients. Solid circles, molecular dynamics simulation, this work; half-filled diamonds, molecular dynamics simulation, ref 26; half-filled triangles, molecular dynamics simulation, ref 27; half-filled squares, molecular dynamics simulation, ref 29; open squares, experimental (ref 4); dashed line, estimated from the SED model.

TABLE 2: Molecular Dynamics Translational and Rotational Diffusion Coefficients

temperature (K)	D_{tr} (10^{-11} m^2 s^{-1})	D_{rot} (10^9 s^{-1})	D_{spin} (10^9 s^{-1})
320	2.49	0.350	0.709
340	6.57	1.20	2.44
360	14.6	2.29	4.83
380	26.6	3.74	8.6
400	38.9	6.01	13.0
420	52.9	8.29	18.5
440	75.6	11.7	27.3
460	114	15.2	34.6
480	126	20.8	42.9

with ratios D_{tr}(molecular dynamics)/D_{tr}(exp) ranging from ~0.65 (high T) to ~1.0 (low T). The authors are aware of three earlier molecular dynamics simulations in which translational diffusion coefficients were computed in liquid OTP. Values obtained in these earlier studies are also plotted in Figure 4 (half-filled symbols). It is interesting to note that in the two investigations in which the Lennard-Jones (LJ) interaction parameters were specifically chosen to match experimental and computed values of D_{tr} at high temperature (at 400 K in ref 26 and over the range 380−440 K in ref 29), the values of D_{tr}(molecular dynamics) at lower temperatures are far higher than experiment, i.e., the predicted dependence on temperature is too shallow. Diffusion constants determined by Kudchadkar and Wiest[27] (half-filled triangles in Figure 4) are relatively close to those found in this study, although their values are somewhat smaller at the lower temperatures studied. The comparatively good agreement between the two simulations is perhaps not too surprising, in that they transferred interaction parameters from benzene, which is similar to the LJ parameter development in the COMPASS force field (vide supra).

It is instructive to compare the experimental and molecular-dynamics-derived diffusion coefficients to those predicted by the classical Stoke−Einstein−Debye (SED)[54] model, D_{tr}(SED) $= k_BT/(\alpha\pi\eta R)$, where η is the solution viscosity and R is the molecular radius. The quantity, α, depends on whether one assumes "stick" ($\alpha = 6$) or "slip" ($\alpha = 4$) boundary conditions. We used the latter value, which is generally found to be more realistic for moderately sized molecules in the neat liquid. Experimental viscosities were computed from the parametric equation determined by Greet and Turnbull[45] (eq 5 and Table 2) from fits of theirs and earlier measured viscosity data. The effective molecular radius, R, was computed by determining the fractional occupied volume via insertion of a large numbers of random points into the cubic cell.[55] It was found that $R =$ 3.82 Å (at all temperatures), in quantitative agreement with the value obtained from van der Waals volume increments.[56] It must be remembered, though, that the SED model assumes spherical molecules. Thus, the value of R must be regarded only as an approximate, effective radius.

Calculated values of D_{tr}(*SED*) are displayed as a function of temperature in Figure 4. As seen in the figure, the theoretical diffusion coefficients are in qualitative agreement with experimental and simulated results. However, given the assumptions inherent in the SED model (e.g., spherical molecules and purely slip boundary conditions), it is not surprising that there are significant quantitative differences between predicted and observed (experiment and simulation) diffusion coefficients.

D. Rotational Diffusion. Molecular dynamics is a powerful tool for investigation of details of the rotational dynamics in molecular liquids. One can monitor the time evolution of various molecule-fixed unit vectors to obtain the first (P_1) or second (P_2) order rotational autocorrelation functions, whose rates of decay are a measure of the rotational diffusion rate of these vectors.[57]

To explore the rotational dynamics in liquid OTP and possible anisotropy of the rates of rotation about various molecular axes, we have monitored the time dependence of three vectors on the central benzene (diagram below): **A** lies along the molecule's C_2 axis (vectors $C_\alpha-C_\beta$ and equivalent vectors); **B** is in the plane of the central benzene but perpendicular to **A** (e.g., $C_\alpha-C_\gamma$); **C** (not shown) is perpendicular to both **A** and **B** and, thus, normal to the plane of the central benzene. In addition, to determine the freedom of internal "spinning" of the two ortho phenyl rings, correlation functions were determined for the vector **I** (e.g., $C_\delta-C_\epsilon$).

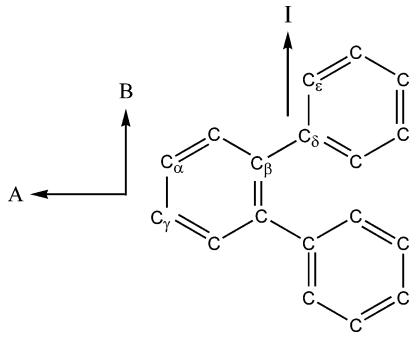

Normalized reorientational correlation functions (CFs), representing decay of the second-order Legendre polynomial, are given by[58]

$$G_\alpha(t) = \langle P_2(t)\rangle = \frac{1}{2}\langle 3\cos^2(\theta(t)) - 1\rangle \quad \alpha = A, B, C, I \qquad (1)$$

where $\theta(t) = \mu(0)\cdot\mu(t)$; μ is a unit vector along the relevant axis (*A*, *B*, *C*, *I*). Values of $G_\alpha(t)$ were determined at 1-ps time increments for these four vectors as a function of temperature by averaging over equivalent vectors on all molecules in the cell and multiple time origins. A representative set of CFs (G_α-(t), $\alpha = A, B, C, I$) at 400 K are displayed on a semilogarithmic plot in Figure 5. One observes a discontinuous drop in the CF

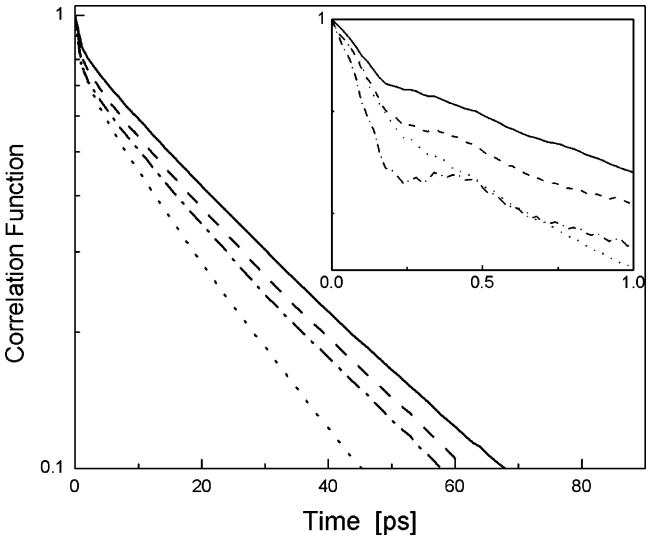

Figure 5. Reorientational correlation functions (at 400 K). Solid line, $G_A(t)$; dashed line, $G_B(t)$; dash-dotted line, $G_C(t)$; dotted line, $G_I(t)$. See text for definitions of vectors *A*, *B*, *C*, *I*.

(from 1 to ~0.65−0.95, depending upon vector and temperature) within the first 1 ps, followed by a more regular decay in succeeding times.

To explore the short-time reorientational motions, CFs were also obtained (from the 5-ps simulations stored at 0.02-ps increments, vide supra) for the first 1-ps interval. As seen in the Figure 5 inset, there is an initial decay, followed by a rise in $G(t)$, which is most notable for G_B and G_C. There have been a number of experimental studies of OTP (dielectric relaxation,[7,8] dynamic light scattering,[9−14] and inelastic neutron scattering[15−19]) in which the results infer the presence of a fast β decay process in superposed on a slow α relaxation, However, the authors believe that the short-time behavior in the rotational CF observed

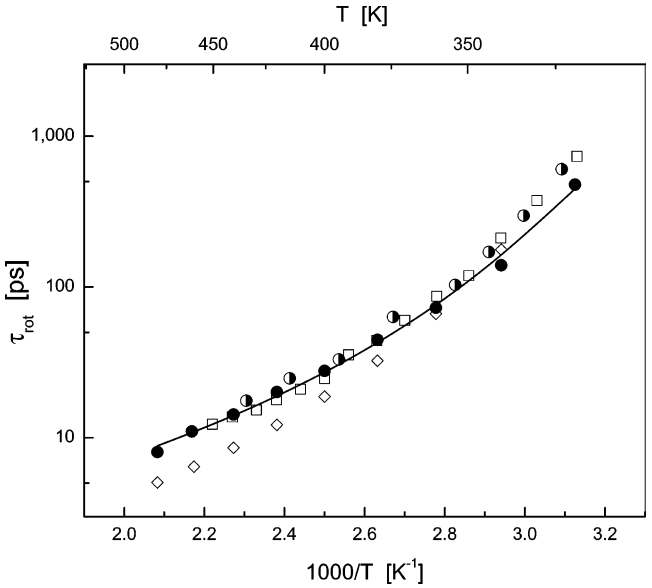

Figure 6. Reorientational correlation times. Solid circles, computed from molecular dynamics simulations; open squares, experimental (determined from ^{2}D NMR relaxation, ref 5); open diamonds, experimental (determined from ^{1}H NMR relaxation, ref 4); half-filled circles, experimental (determined from light scattering, ref 12); solid curve, fit of molecular dynamics times by the VFT equation.

here is, instead, the result of a brief period (<0.2 ps) of free rotation (in which the correlation function is predicted to be approximately Gaussian in character[59,60]) followed by a collision-induced reversal in the direction of rotation. This is consistent with the result of another simulation of OTP, in which Kudchadkar and Wiest[27] report a reversal in the linear velocity autocorrelation function at ~0.2−0.4 ps (Figure 6 of the reference), which they attribute to a reversal of translational motion upon collision with a neighboring molecule in the "solvent" cage.

From the figure, one finds the decay is initially nonexponential (nonlinear on a semilogarithmic scale), indicating a distribution of correlation times in the liquid. After the first 10−20 ps, decay in the CFs become exponential in time. To derive reorientational correlation times, τ_α ($\alpha = A, B, C, I$), the CFs were fit (in the region from 1 ps to times at which $G_\alpha(t) \approx 0.1$) by the Kohlrausch−Williams−Watts (KWW) stretched exponential function[61−63]

$$G_\alpha(t) = \exp[(-t/\tau_\alpha)^\beta] \tag{2}$$

In this expression, τ_α is the KWW correlation time and β is the distribution parameter (values of $\beta \ll 1$ represent a broad distribution of correlation times). The derived values of τ_α and β (which varied from 0.75 to 0.90) were then used in the following equation to obtain the effective mean correlation time for the distribution, given by

$$\langle \tau_a \rangle = \tau_\alpha \cdot \frac{\Gamma(\beta^{-1})}{\beta} \tag{3}$$

where Γ is the Gamma function. The derived rotational correlation times are given in Table 3. One observes from the table that, at all temperatures, $\tau_A > \tau_B > \tau_C$. However, the differences are comparatively small; the ratio τ_A/τ_C is in the range from 1.1 to 1.2 at all temperatures. Because the correlation times for rotation of the three orthogonal molecule-fixed vectors are close to equal, it can be concluded that, despite the fact that OTP is an asymmetric top with significantly different semiaxis lengths,[64] that there is very little anisotropy in its overall reorientational dynamics in the liquid. In contrast, the ratio of correlation times of the equivalent vectors in liquid benzene is much higher,[65−68] indicating a significantly greater rotational anisotropy.

TABLE 3: Reorientational Correlation Times[a]

temperature (K)	τ_A (ps)	τ_B (ps)	τ_C (ps)	τ_I (ps)
320	508	474	448	356
340	145	140	132	103.5
360	76.8	72.4	69.0	53.3
380	47.5	44.8	41.4	31.4
400	29.5	27.3	26.4	20.1
420	21.5	20.0	18.7	14.3
440	15.2	14.6	13.0	9.96
461	11.8	11.09	10.09	7.76
480	8.75	8.05	7.27	5.94

[a] See text for definition of correlation times.

The temperature dependence of the average of the three correlation times in OTP is displayed in an Arrhenius plot in Figure 6. It is convenient to represent the computed rotational times parametrically. Therefore, we have fit the data to the Vogel−Fulcher−Tamman (VFT) equation,[69] $\tau = \tau_0 \cdot \exp[DT_0/(T - T_0)]$, which is shown as the solid curve in the figure. The fitted value of D is 3.22 ($\tau_0 = 0.66$ ps, $T_0 = 214$ K), which is well below the commonly taken "crossover" value of $D \approx 10$, under which the substance is considered to be a fragile glass former and exhibits non-Arrhenius behavior.[1] However, it should be noted that truly meaningful VFT parameters in OTP requires data over a much broader range of temperature, and approaching significantly closer to T_g.

The measurement of NMR relaxation times is the most commonly used technique for experimental determination of rotational correlation times in liquids. There have been at least two NMR investigations of reorientation of OTP over an extended range of temperature, by ^{1}H dipole−dipole relaxation[4] and ^{2}D quadrupolar relaxation (in OTP-d_{18}).[5,70] Correlation times from both studies are displayed in Figure 6. One observes that results of the two measurements are in good agreement at lower temperatures, although values of $\tau_{rot}(^1H)$ are somewhat lower than $\tau_{rot}(^2D)$ at the higher temperatures studied. It is satisfying to note from the figure that rotational times derived from the MD simulations are in very good agreement with the experimental data (particularly $\tau_{rot}(^2D)$) over a two-decade range of values. The computed correlation times also exhibit the non-Arrhenius behavior observed experimentally, although they rise a bit more slowly at the two lowest temperatures. Our recent molecular dynamics simulation of benzene revealed no deviations of the reorientational dynamics from Arrhenius behavior over its complete liquid range.[53]

Of course, it would be very useful to explore the reorientational (and translational) dynamics of OTP at temperatures closer to its glass transition temperature (243 K) to characterize the motional behavior in the vicinity of T_g. Unfortunately, unlike some experimental techniques (notably NMR relaxation and dynamic light scattering), current constraints on current computer processing speeds makes it unfeasible to perform molecular dynamics simulations longer than on the order of 20−30 ns (with our facilities, calculations on OTP require approximately 1 day for each 1 ns of simulation time). On the basis of data from the ^{2}D NMR investigation of OTP,[5] a decrease of even 20 K in temperature (to 300 K) increases the reorientational correlation time by a factor of 10 (to ~8 ns), which would require a simulation of at least ~50 ns to determine the correlation function. A further 20 K decrease in temperature to

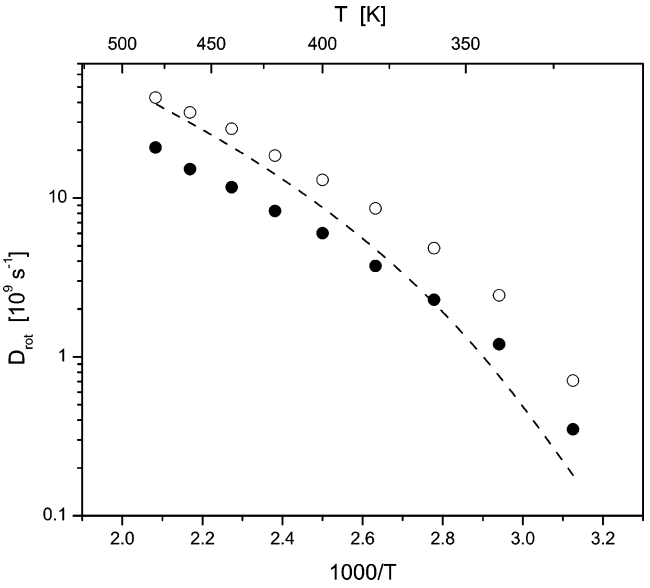

Figure 7. Computed reorientational diffusion coefficients. Solid circles, D_{rot}; open circles, D_{spin}; dashed line, estimate of D_{rot} from microviscosity model.

280 K (still far above T_g) would increase τ_{rot} by an additional 2 orders of magnitude.

It was discussed above that reorientational correlation times derived from vectors fixed on the molecular skeleton are very close in magnitude at all temperatures, indicating isotropic overall rotation. However, from Figure 5, one observes that $G_l(t)$ decays significantly more rapidly than the correlation functions of vectors *A*, *B*, and *C*, and consequently, the correlation times, τ_l, are shorter for vector *I* at all temperatures (Table 3). Unlike *A*, *B*, and *C*, the rotation of *I* is affected both by overall tumbling of the molecule and internal "spinning" of the phenyl groups relative to the molecular skeleton. The rotational correlation time for this vector can be related to the overall tumbling and internal spinning diffusion coefficients, D_{rot} and D_{spin}, via the standard equation[71,72]

$$\tau(\theta) = \frac{\frac{1}{4}(3\cos^2\theta - 1)^2}{6D_{rot}} + \frac{3\sin^2\theta\cos^2\theta}{5D_{rot} + D_{spin}} + \frac{\frac{3}{4}\sin^4\theta}{2D_{rot} + 4D_{spin}} \quad (4)$$

To apply this equation, we have assumed that the overall rotation is isotropic, with a diffusion constant determined from the average overall rotation time (average of τ_A, τ_B, and τ_C in Table 3) via $D_{rot} = (6\tau_{rot})^{-1}$. The internal rotation axis is taken to be the bond connecting each pendant phenyl ring to the central benzene ($C_\beta - C_\delta$ in the diagram above). As noted earlier, the vector *I* which was used to monitor internal rotation is $C_\delta - C_\epsilon$ in the diagram. θ is the angle between this vector and the internal rotation axis (120°). We have used values of D_{rot} and τ_l in this equation with $\theta = 120°$ to determine D_{spin} as a function of temperature. The two rotational diffusion coefficients are contained in Table 2 and plotted in Figure 7.

One observes that $D_{spin} > D_{rot}$ (by factors ranging from 2.0 to 2.3) at all temperatures, indicating significant internal rotation of the phenyl groups; if these groups were rigid, it would correspond to $D_{spin} = 0$. It is not really surprising that one finds relatively free spinning of the lateral phenyl groups in OTP. A simple relaxed scan of the dihedral angle of one phenyl (allowing the other to rotate out of the way) using the semiempirical AM1 method[73] reveals that there is a very low barrier to internal rotation over a wide range of angle (from 30 to 150°), for which the total variation in the energy is ~5 kJ mol^{-1}. The relatively free internal rotation of the phenyl groups found here is consistent with the NMR results of Sillescu and co-workers,[5] who interpreted their low temperature ^{2}D spin-alignment experiments as indicating relatively large "flips" of the phenyl groups (by ~60°) even in the glassy regime, where the overall molecular orientation is essentially frozen.

Finally, we have computed overall rotational diffusion coefficients using the Gierer−Wirtz microviscosity model,[74] $D_{rot} = k_B T/(8\pi\eta R^3 f)$. For pure liquids, the microviscosity factor, $f = (6.125)^{-1}$. We have used the approximate value of R (3.82 Å) derived above and experimental viscosities from the parametric equation in ref 45. Noting the dependence of D_{rot} on R^{-3}, the assumption of spherical molecules and the applicability of the microviscosity boundary conditions,[74] limits the applicability of this model to qualitative comparisons.

As shown in the figure, one finds acceptable qualitative agreement with rotational diffusion coefficients determined from the molecular dynamics simulations, D_{rot}(molecular dynamics). However, as observed earlier for translational diffusion, values of D_{rot} from this viscosity based model exhibit a steeper dependence on temperature than those obtained from the simulations (and from experiment).

Summary and Conclusions

Molar volumes of the fragile glass-forming liquid, OTP, computed using the COMPASS force field were in very good agreement with experiment over a 160 K range of temperature. Enthalpies of vaporization derived from calculated cohesive energy densities agreed qualitatively with experiment (within 7−8%) and exhibited the same dependence upon temperature.

The computed translational diffusion coefficients were in good semiquantitative agreement with experimental values and demonstrated a non-Arrhenius temperature dependence, similar to experimental observations.

Reorientational correlation functions were measured for three vectors fixed relative to the central benzene ring as well as for a vector in the lateral phenyl groups. The correlation functions exhibited a very short initial (<1 ps) decay superposed on a much slower decrease in the functions, reflecting a short period of free-rotor-type rotation prior to collision of the molecule with neighbors in its solvent shell. Derived rotational correlation times of the three molecule-fixed vectors were close to equal at all temperatures, revealing that the overall molecular rotation in liquid OTP is close to isotropic. These correlation times exhibit the same non-Arrhenius behavior and were in excellent semiquantitative agreement with experimental times derived from ^{2}D and ^{1}H relaxation.

Data from all four vectors were used to compute overall (D_{rot}) and internal "spinning" (D_{spin}) rotational diffusion coefficients. It was found that $D_{spin} > D_{rot}$ (by approximately a factor of 2.5), reflecting the relatively free internal rotation of phenyl groups in the liquid.

From the results of this study, we conclude that molecular dynamics simulations using the COMPASS force field properly capture the non-Arrhenius behavior of the dynamical properties in glass-forming liquids and can be used to provide reasonably accurate estimates of the translational and rotational diffusion coefficients in these interesting fluids.

Acknowledgment. The authors acknowledge the AFRL Materials and Manufacturing Directorate and the ASC and ARL Major Shared Resource Centers, operated by the DoD High

Performance Computing Modernization Office. One of the authors (M.S.) thanks the Robert A. Welch Foundation (Grant B-657) and the Universal Technology Corporation for financial support. This project was conducted under a Cooperative Research and Development Agreement (CRDA 04-306-ML-01) between AFRL and Accelrys, Inc., for the development and validation of the COMPASS force field. One of the authors (M.S.) wishes to thank Dr. William E. Acree, Jr., for helpful discussions concerning the accurate treatment of experimental vapor pressure data.

References and Notes

(1) Angell, C. A. Fragile Glass Formers. In *Relaxation in Complex Systems*; Ngai, K. L., Wright, G. B., Eds.; Office of Naval Research: Washington, D.C., 1984; p 3.
(2) Angell, C. A. *J. Phys. Chem.* **1988**, *49*, 863.
(3) Angell, C. A. *Science* **1995**, *267*, 1924.
(4) McCall, D. W.; Douglass, D. C.; Falcone, D. R. *J. Chem. Phys.* **1969**, *50*, 3839.
(5) Dries, T.; Fujara, F.; Kiebel, M.; Rossler, E.; Sillescu, H. *J. Chem. Phys.* **1988**, *88*, 2139.
(6) Schnauss, W.; Fujara, F.; Sillescu, H. *J. Chem. Phys.* **1992**, *97*, 1376.
(7) Johari, G. P.; Goldstein, M. *J. Chem. Phys.* **1970**, *53*, 2372.
(8) Wu, L.; Nagel, S. R. *Phys. Rev. B* **1992**, *46*, 11198.
(9) Fytas, G.; Wang, C. H.; Lilge, D.; Dorfmuller, T. *J. Chem. Phys.* **1981**, *75*, 4247.
(10) Fytas, G.; Dorfmuller, T.; Wang, C. H. *J. Phys. Chem.* **1983**, *87*, 5041.
(11) Gerharz, B.; Meier, G.; Fischer, E. W. *J. Chem. Phys.* **1990**, *92*, 7110.
(12) Steffen, W.; Patkowski, A.; Meier, G.; Fischer, E. W. *J. Chem. Phys.* **1992**, *96*, 4171.
(13) Fischer, E. W.; Meier, G.; Rabenau, T.; Patkowski, A.; Steffen, W. *J. Non-Cryst. Solids* **1991**, *131*−*133*, 134.
(14) Fischer, E. W.; Donth, E. *Phys. Rev. Lett.* **1992**, *68*, 2344.
(15) Bartsch, E.; Fujara, F.; Kiebel, M.; Sillescu, H.; Petry, W. *Ber. Bunsen-Ges. Phys. Chem.* **1989**, *93*, 1252.
(16) Bartsch, E.; Debus, O.; Fujara, F.; Kiebel, M.; Sillescu, H.; Petry, W. *Ber. Bunsen-Ges. Phys. Chem.* **1991**, *95*, 1146.
(17) Petry, W.; Bartsch, E.; Fujara, F.; Kiebel, M.; Sillescu, H.; Farago, B. *Z. Phys. B* **1991**, *83*, 175.
(18) Debus, O.; Zimmermann, H.; Bartsch, E.; Fujara, F.; Kiebel, M.; Petry, W. *Chem. Phys. Lett.* **1991**, *180*, 271.
(19) Fujara, F.; Geil, B.; Sillescu, H.; Fleischer, G. *Z. Phys. B* **1992**, *88*, 195.
(20) Chang, I.; Fujara, F.; Geil, B.; Heuberger, G.; Mangel, T.; Sillescu, H. *J. Non-Cryst. Solids* **1994**, *172*−*174*, 248.
(21) Cicerone, M. T.; Blackburn, F. R.; Ediger, M. D. *J. Chem. Phys.* **1995**, *102*, 471.
(22) Cicerone, M. T.; Ediger, M. D. *J. Chem. Phys.* **1995**, *103*, 5684.
(23) Cicerone, M. T.; Ediger, M. D. *J. Chem. Phys.* **1996**, *104*, 7210.
(24) Earle, K. A.; Moscicki, J. K.; Polimeno, A.; Freed, J. H. *J. Chem. Phys.* **1997**, *106*, 9996.
(25) Lewis, L. J.; Wahnström, G. *Solid State Commun.* **1993**, *86*, 295.
(26) Lewis, L. J.; Wahnström, G. *Phys. Rev. E* **1994**, *50*, 3865.
(27) Kudchadkar, S. R.; Wiest, J. M. *J. Chem. Phys.* **1995**, *103*, 8566.
(28) Ou, J. J.; Chen, S. H. *J. Computat. Chem.* **1998**, *19*, 86.
(29) Mossa, S.; Di Leonardo, R.; Ruocco, G.; Sampoli, M. *Phys. Rev. E* **2000**, *62*, 612.
(30) Mossa, S.; Ruocco, G.; Sampoli, M. *Phys. Rev. E* **2001**, *64*, 021511.
(31) Accelrys, Inc., San Diego, CA 92121-3752
(32) Sun, H.; Rigby, D. *Spectrochim. Acta, Part A* **1997**, *53*, 1301.
(33) Rigby, D.; Sun, H.; Eichinger, B. E. *Polym. Int.* **1997**, *44*, 311.
(34) Sun, H. *J. Phys. Chem. B.* **1998**, *102*, 7338.
(35) Rigby, D. *Fluid Phase Equilib.* **2004**, *217*, 77.
(36) Aikawa, S.; Maruyama, Y.; Ohashi, Y.; Sasada, Y. *Acta Crystallogr.* **1978**, *B34*, 2901.
(37) Brown, G. M.; Levy, H. A. *Acta Crystallogr.* **1979**, *B35*, 785.
(38) Grumadas, A. J.; Poshkus, D. P.; Kiselev, A. V. *J. Chem. Soc., Faraday Trans. 2* **1982**, *78*, 2013.
(39) Le Fèvre, R. J. W.; Sundaram, A.; Sundaram, K. M. S. *J. Chem. Soc.* **19653**, 3180.
(40) Kobayashi, T. *Bull. Chem. Soc. Jpn.* **1983**, *56*, 3224.
(41) Buxing, W. R. *J. Am. Chem. Soc.* **1982**, *104*, 4829.
(42) Baranovic, G.; Bistricic, L.; Volovšek, L.; Kirin, D. *Mol. Phys.* **2001**, *99*, 33.
(43) Baraldi, I. *THEOCHEM* **1985**, *122*, 287.
(44) Kirin, D.; Volovšek, L.; Pick, R. M. *J. Mol. Struct.* **1999**, *482*−*483*, 421.
(45) Greet, R. J.; Turnbull, D. *J. Chem. Phys.* **1967**, *46*, 1243.
(46) Opdycke, J.; Dawson, J. P.; Clark, R. K.; Dutton, M.; Ewing, J. J.; Schmidt, H. H. *J. Phys. Chem.* **1964**, *68*, 2385.
(47) Rigby, D. Unpublished results.
(48) Sasse, K.; N'Guimbi, J.; Jose, J.; Merlin, J. C. *Thermochim. Acta* **1989**, *146*, 53.
(49) Verevkin, S. P. *J. Chem. Thermodyn.* **1997**, *29*, 1495.
(50) Reiter, V. F. W.; Kind, W.; Nehren, R. *Ber. Bunsen-Ges. Gesellschaft* **1970**, *74*, 462.
(51) Stephenson, R. M.; Malanowski, S. *Handbook of the Thermodynamics of Organic Compounds*; Elsevier: New York, 1987.
(52) Chickos, J. S.; Acree, W. E., Jr. *J. Phys. Chem. Ref. Data* **2003**, *32*, 519.
(53) Schwartz, M.; Duan, D.; Berry, R. J. *J. Phys. Chem. A* **2005**, *109*, 8637.
(54) Stokes, G. *Trans. Cambridge Philos. Soc.* **1953**, *9*, 5.
(55) Bharadwaj, R. K.; Boyd, R. H. *Polymer* **1999**, *40*, 4229.
(56) Bondi, A. *J. Phys. Chem.* **1964**, *68*, 441.
(57) Haile, J. M. *Molecular Dynamics Simulation: Elementary Methods*; John Wiley & Sons: New York, 1992.
(58) Lindsey, C. P.; Patterson, G. D. *J. Chem. Phys.* **1980**, *73*, 3348.
(59) Steele, W. A. *J. Chem. Phys.* **1963**, *38*, 2411.
(60) Steele, W. A. *Mol. Phys.* **1981**, *43*, 141.
(61) Williams, G.; Watts, D. C. *Trans. Faraday Soc.* **1970**, *66*, 80.
(62) Jäckle, J. *Rep. Prog. Phys.* **1986**, *49*, 171.
(63) Phillips, J. C. *Rep. Prog. Phys.* **1996**, *59*, 1133.
(64) Andrews, J. N.; Ubbelohde, A. R. *Proc. R. Soc.* **1955**, *A228*, 435.
(65) Dölle, A.; Suhm, M. A.; Weingärtner, H. *J. Chem. Phys.* **1991**, *94*, 3361.
(66) Python, H.; Mutzenhardt, P.; Canet, D. *J. Phys. Chem. A* **1997**, *101*, 1793.
(67) Laaksonen, A.; Stilbs, P.; Wasylishen, R. E. *J. Chem. Phys.* **1998**, *108*, 455.
(68) Witt, R.; Sturz, L.; Dölle, A.; Müller-Plathe, F. *J. Phys. Chem. A* **2000**, *104*, 5716.
(69) Angell, C. A. *J. Non-Cryst. Solids* **1991**, *131*−*133*, 13.
(70) Rotational correlation times were obtained by digitization of Figure 2 of ref XX, followed by numerical interpolation.
(71) Woessner, D. E. *J. Chem. Phys.* **1962**, *36*, 1.
(72) Woessner, D. E. *J. Chem. Phys.* **1962**, *37*, 647.
(73) Dewar, M. J. S.; Zoebisch, E. G.; Healy, E. F.; Stewart, J. J. P. *J. Am. Chem. Soc.* **1985**, *107*, 3902.
(74) Gierer, A.; Wirtz, K. *Z. Naturforsch., A* **1953**, *8*, 532.